

General Disclaimer

One or more of the Following Statements may affect this Document

- This document has been reproduced from the best copy furnished by the organizational source. It is being released in the interest of making available as much information as possible.
- This document may contain data, which exceeds the sheet parameters. It was furnished in this condition by the organizational source and is the best copy available.
- This document may contain tone-on-tone or color graphs, charts and/or pictures, which have been reproduced in black and white.
- This document is paginated as submitted by the original source.
- Portions of this document are not fully legible due to the historical nature of some of the material. However, it is the best reproduction available from the original submission.

NATIONAL AERONAUTICS AND SPACE ADMINISTRATION

Technical Memorandum 33-781

*The Transient Thermal Response of a
Tubular Solar Collector*

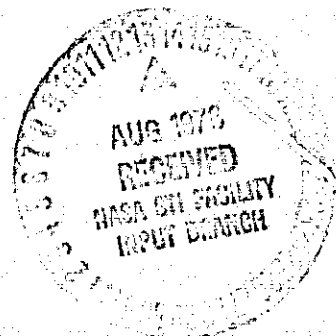
(NASA-CR-148488) THE TRANSIENT THERMAL
RESPONSE OF A TUBULAR SOLAR COLLECTOR (Jet
Propulsion Lab.) 44 p HC \$4.00 CSCL 10A

N76-28649

Unclas
G3/44 47646

JET PROPULSION LABORATORY
CALIFORNIA INSTITUTE OF TECHNOLOGY
PASADENA, CALIFORNIA

July 15, 1976



1. Report No. 33-781	2. Government Accession No.	3. Recipient's Catalog No.	
4. Title and Subtitle THE TRANSIENT THERMAL RESPONSE OF A TUBULAR SOLAR COLLECTOR		5. Report Date July 15, 1976	
		6. Performing Organization Code	
7. Author(s) F. L. Lansing		8. Performing Organization Report No.	
9. Performing Organization Name and Address JET PROPULSION LABORATORY California Institute of Technology 4800 Oak Grove Drive Pasadena, California 91103		10. Work Unit No.	
		11. Contract or Grant No. NAS 7-100	
		13. Type of Report and Period Covered Technical Memorandum	
12. Sponsoring Agency Name and Address NATIONAL AERONAUTICS AND SPACE ADMINISTRATION Washington, D.C. 20546		14. Sponsoring Agency Code	
15. Supplementary Notes			
16. Abstract This article is a continuation and an extension to the previous work covered in Ref. (1) that deals with the thermal behavior of a tubular solar collector. A special analytical solution is provided for the time-wise response of the circulating fluid temperatures when a sudden step change of the input solar radiation is imposed and remains constant thereafter. An example which demonstrates the transient temperatures at the exit section of a single collector with two different flow patterns is presented. This study is used to supplement some numerical solutions to provide a fairly complete coverage for this type of solar collector.			
17. Key Words (Selected by Author(s)) Fluid Mechanics and Heat Transfer Energy Production and Conversion Systems Analysis Solar Physics		18. Distribution Statement Unclassified -- Unlimited	
19. Security Classif. (of this report) Unclassified	20. Security Classif. (of this page) Unclassified	21. No. of Pages 38	22. Price

HOW TO FILL OUT THE TECHNICAL REPORT STANDARD TITLE PAGE

Make items 1, 4, 5, 9, 12, and 13 agree with the corresponding information on the report cover. Use all capital letters for title (item 4). Leave items 2, 6, and 14 blank. Complete the remaining items as follows:

3. Recipient's Catalog No. Reserved for use by report recipients.
7. Author(s). Include corresponding information from the report cover. In addition, list the affiliation of an author if it differs from that of the performing organization.
8. Performing Organization Report No. Insert if performing organization wishes to assign this number.
10. Work Unit No. Use the agency-wide code (for example, 923-50-10-06-72), which uniquely identifies the work unit under which the work was authorized. Non-NASA performing organizations will leave this blank.
11. Insert the number of the contract or grant under which the report was prepared.
15. Supplementary Notes. Enter information not included elsewhere but useful, such as: Prepared in cooperation with... Translation of (or by)... Presented at conference of... To be published in...
16. Abstract. Include a brief (not to exceed 200 words) factual summary of the most significant information contained in the report. If possible, the abstract of a classified report should be unclassified. If the report contains a significant bibliography or literature survey, mention it here.
17. Key Words. Insert terms or short phrases selected by the author that identify the principal subjects covered in the report, and that are sufficiently specific and precise to be used for cataloging.
18. Distribution Statement. Enter one of the authorized statements used to denote releasability to the public or a limitation on dissemination for reasons other than security of defense information. Authorized statements are "Unclassified-Unlimited," "U. S. Government and Contractors only," "U. S. Government Agencies only," and "NASA and NASA Contractors only."
19. Security Classification (of report). NOTE: Reports carrying a security classification will require additional markings giving security and downgrading information as specified by the Security Requirements Checklist and the DoD Industrial Security Manual (DoD 5220.22-M).
20. Security Classification (of this page). NOTE: Because this page may be used in preparing announcements, bibliographies, and data banks, it should be unclassified if possible. If a classification is required, indicate separately the classification of the title and the abstract by following these items with either "(U)" for unclassified, or "(C)" or "(S)" as applicable for classified items.
21. No. of Pages. Insert the number of pages.
22. Price. Insert the price set by the Clearinghouse for Federal Scientific and Technical Information or the Government Printing Office, if known.

NATIONAL AERONAUTICS AND SPACE ADMINISTRATION

Technical Memorandum 33-781

*The Transient Thermal Response of a
Tubular Solar Collector*

F. L. Lansing

JET PROPULSION LABORATORY
CALIFORNIA INSTITUTE OF TECHNOLOGY
PASADENA, CALIFORNIA

July 15, 1976

PREFACE

The work described in this report was performed by the Telecommunications Division of the Jet Propulsion Laboratory.

Table of Contents

Introduction	1
Collector Description and Flow Patterns	2
Assumptions and Analysis	2
Numerical Example	4
Summary and Conclusions	8
Nomenclatures	11
References	13
Appendix A	17
Appendix B	23
Appendix C	30
Appendix D	36

List of Figures

Fig. 1a. Collector configuration (flow pattern 1)	14
Fig. 1b. Temperature distribution along one collector (flow pattern 1) at time θ	14
Fig. 2a. Collector configuration (flow pattern 2)	14
Fig. 2b. Temperature distribution along one collector (flow pattern 2) at time θ	14
Fig. 3. Two collector tubes in series	15
Fig. 4. Transient response of the outlet fluid temperature of the tubular solar collector as derived from the analysis	16
Fig. A-1 Sankey Diagram for the Tubular Solar Collector	22
Fig. B-1 Step change in the solar radiation at $\theta = 0$	29
Fig. B-2 Step change in the parameter K_4	29

Abstract

This article is a continuation and an extension to the previous work covered in Ref. (1) that deals with the thermal behavior of a tubular solar collector. A special analytical solution is provided for the time-wise response of the circulating fluid temperatures when a sudden step change of the input solar radiation is imposed and remains constant thereafter. An example which demonstrates the transient temperatures at the exit section of a single collector with two different flow patterns is presented. This study is used to supplement some numerical solutions to provide a fairly complete coverage for this type of solar collector.

The Transient Thermal Response of a Tubular Solar Collector

Introduction

The study of transition states in the performance of solar collectors is becoming increasingly important with the new introduction of solar module control techniques. The temperature control versus the circulating fluid rate, for example, is directly related to the transient behavior of the module at specific input conditions of solar irradiancy, ambient and inlet fluid temperatures.

In order to study the transient performance of any heat exchanger, a sufficiently general analytical model must be established which is both an adequate idealization of the physical system and capable of reasonably simple mathematical description. There are basically three common methods in the literature for solving the transient performance problem. These are classified as: an analog computer method, a numerical method, and an analytical method. The choice of the method to be used depends on the complexity and size of the problem, the accuracy required, the means available, and the experience of the investigator. First, analog computer methods (Ref. 3, 4 & 5) provide a realistic and accurate analog model of the physical system, but require a significant amount of advanced electrical circuitry. Second, numerical solutions employing the practical method of finite differences has become increasingly popular with the availability of high speed digital computers and its associated technology. This technique is very useful for almost any heat exchanger problem, and is the only method that can be used if a high degree of accuracy is required or if the problem at hand is of considerable size and complexity. One using this method has to solve algebraic equations (nodal equations) instead of the partial differential equation. The nodal equations can be derived

by purely mathematical methods or by energy considerations. Third, analytical methods, as evident from Ref. 2, present in general a substantial mathematical complexity. However, a special case has been found for tubular solar collectors which can be handled by standard procedures and this is the subject of this article. The analytic solution of the transient behavior can later be used to supplement the numerical solutions so as to provide adequate coverage for this type of solar collector.

Collector Description and Flow Patterns

The tubular collector, as shown schematically in Figures 1 and 2, is composed of three concentric tubes; an inner tube, an absorber tube, and a cover tube. The annulus space between the absorber and cover tubes is highly evacuated to minimize convection and conduction losses. The absorber tube surface is coated with a selective material to reduce the outward long-wave radiation losses. In flow pattern (1), as shown in Figure 1, the circulating fluid starts from the inlet section of the inner tube. At the closed end of the collector, the fluid reverses its direction and passes in the annulus spacing between the inner and absorber tubes. In flow pattern (2), as shown in Figure 2, the fluid path is reversed from the above. Both flow patterns alternate in each collector module as shown in Figure 3. For more irradiancy augmentation, the set of collectors is mounted with lateral spaces separating them from each other with a highly reflective back reflector.

Assumptions and Analysis

It is widely recognized that the analysis of the transition states of heat exchangers does not respond to an easy mathematical treatment, and that simplifying assumptions are necessary in order to achieve any type of solution.

The following idealizations are made in the model to yield a transient solution with an accuracy adequate for engineering purposes:

- 1 - The heat flux and the temperature of each of the fluids and the walls are functions of both time (θ) and axial distance (X) from the collector inlet. This makes the problem one dimensional.
- 2 - The densities and specific heats are constants throughout the system.
- 3 - The thermal conduction of the tubes' material is assumed zero in the axial direction parallel to the flow and is considered infinite in the radial direction.
- 4 - The heat transfer coefficient between any tube surface and its adjacent fluid is uniform and constant over the axial direction for a fixed fluid flow rate.
- 5 - The heat transferred at any section due to the fluid thermal conductivity in the axial direction, within the fluid, is negligible compared to other heat fluxes from or to the fluid at the same section.
- 6 - The heat capacitance of the three tubes of the collector, namely the inner, the absorber and the cover tube, are negligible relative to the heat capacity of the fluid. This is a good simplifying assumption if a liquid is used as the circulating fluid in the collector. In case of using gases or air as the solar collector medium, this assumption is not recommended since the wall capacitance has large effects on the thermal lag.
- 7 - Initially, steady state conditions were prevailing before a sudden input variation in the solar radiation was superimposed.
- 8 - The fluid flow rate is constant throughout the collector.
- 9 - Passes (1) and (2) of the inner and outer fluid, respectively, are of equal flow area; thus equal flow velocities in each pass are assumed.

Virtually all of these idealizations are also required for the analysis of the steady state performance.

Based upon these idealizations, the differential equations relating the system temperatures are derived from energy balance and heat transfer rate equations applied to a segment of the collector of length dx . The derivation of these differential equations is presented in Appendix A. The incident solar radiation is then applied in the form of an input step function. The transient problem for both flow patterns is then mapped on the frequency domain instead of the time domain by using Laplace transformation as explained in Appendix B. In Appendix C, the inverse Laplace transformation is presented using the Residue theorem in complex number algebra, for one of the two flow patterns, namely pattern (1). A similar approach is followed for flow pattern (2) and is presented separately in Appendix D.

Numerical Example

The following numerical example will show the difference in the thermal response between the two flow patterns of the tubular solar collector. The data were arbitrarily abstracted to be as close as possible to actual running conditions. However, the conclusions may be generalized at any other relevant conditions.

Starting with inlet water temperature

$$T_i(0,0) = 70^{\circ}\text{C for flow pattern (1)}$$

or

$$T_o(0,0) = 70^{\circ}\text{C for flow pattern (2)}$$

Ambient temperature 30⁰c
 Tube length 1.067m
 Absorber tube diameter . . . 0.041m
 Cover tube transmissivity . . 0.91
 Absorber tube absorptivity . . 0.85
 Mass flow rate. 5 Kg/hr
 Water specific heat 11.63 x 10⁻⁴ Kw/hr/Kg⁰K
 Sky temperature 4⁰c
 Leader tube diameter 0.029m
 Cover tube diameter 0.051m
 Cover tube emissivity 0.90
 Absorber tube emissivity. . . 0.1
 Wind speed 11 Km/hr
 Augmentation factor 1.64

Irradiation intensity varies in the form of a step function and is given by

$$I = \begin{cases} 0 & \theta < 0 \\ 0.75 \text{ Kw/m}^2 & 0 \leq \theta < \infty \end{cases}$$

The relevant constants K_1 , K_3 , K_4 (θ) were calculated from Eqs. A-20 & A-23 using the heat transfer coefficients data (Ref. 6):

$$K_1 = 0.8853 \text{ m}^{-1} \qquad K_4 = \begin{cases} 5.0869 & \theta < 0 & \text{ }^{\circ}\text{K/m} \\ 13.4406 & 0 \leq \theta < \infty & \text{ }^{\circ}\text{K/m} \end{cases}$$

$$K_3 = 0.9024 \text{ m}^{-1}$$

$$\Delta K_4 (\theta=0) = 8.3537 \text{ }^{\circ}\text{K/m}$$

$$C = \frac{(K_3 - K_1)}{2} = 0.0085495$$

$$V_i = V_o = V = 7.5698 \text{ m/hr}$$

Since the initial conditions were at steady state, Equation B-9 was solved as in Ref. (1) and gave the difference $[T_o(0,0) - T_i(0,0)]$ as -0.818 ⁰K

The first six vectors Z in Equation C-17 and the corresponding poles p are calculated as:

$$\begin{array}{ll}
 Z = \pm 1.8274 j & , \quad p = -5.0655 \\
 Z = 2.1065 \pm 7.5750 j & , \quad p = -14.4634 \mp 26.0865 j \\
 Z = 2.7063 \pm 13.9438 j & , \quad p = -16.4525 \mp 49.0227 j \\
 Z = 3.0754 \pm 20.2691 j & , \quad p = -17.7222 \mp 71.5935 j \\
 Z = 3.3437 \pm 26.5781 j & , \quad p = -18.6569 \mp 94.0439 j \\
 Z = 3.5548 \pm 32.8788 j & , \quad p = -19.3968 \mp 116.4385 j
 \end{array}$$

The first six poles constitute 97% of the infinite series sum required for flow pattern (1) and are sufficient for temperature calculations. For flow pattern (2) many more transition terms are required for calculations in the vicinity of the ($\theta = 0$) region. These extra terms will have a very rapid diminishing effect as $\theta \geq 0.1$ hr.

The temperature $T_0(0, \theta)$, from Equation C-16, for flow pattern (1) is given by:

$$\begin{aligned}
 T_0(0, \theta) = T_0(0, 0) + 8.7826 - 6.5290 e^{-5.0655 \theta} \\
 + 2.7288 e^{-14.4634 \theta} \cdot \cos(2.1593 + 26.0865 \theta) \\
 + 0.4480 e^{-16.4525 \theta} \cdot \cos(1.5462 - 49.0227 \theta) \\
 + 0.5363 e^{-17.7222 \theta} \cdot \cos(2.3276 + 71.5935 \theta) \\
 + 0.1964 e^{-18.6569 \theta} \cdot \cos(1.2973 - 94.0439 \theta) \\
 + 0.2447 e^{-19.3968 \theta} \cdot \cos(2.3688 + 116.4385 \theta)
 \end{aligned}$$

and that for flow pattern (2), from Equation D- 9, is given by:

$$\begin{aligned}
 T_i(0,\theta) = T_i(0,0) + & 8.7826 - 14.6569 e^{-5.0655 \theta} \\
 & + 2.9974 e^{-14.4634 \theta} \cos(1.7492 - 26.0865 \theta) \\
 & + 1.0818 e^{-16.4525 \theta} \cos(2.0444 - 49.0227 \theta) \\
 & + 1.0681 e^{-17.7222 \theta} \cos(1.6352 - 71.5935 \theta) \\
 & + 0.6108 e^{-18.6569 \theta} \cos(1.8797 - 94.0439 \theta) \\
 & + 0.5429 e^{-19.3968 \theta} \cos(1.6005 - 116.4385 \theta)
 \end{aligned}$$

The outlet temperatures are plotted as shown in Fig. 4 for both flow patterns. The trend of the two outlet temperature curves is the same for any other conditions of flow rate, ambient temperature or solar irradiancy.

Summary and Conclusions

To summarize the major features of this work the following conclusions are made:

- 1 - A pure analytic procedure using Laplace transform has been established for the transient thermal solution of the tubular solar collector with two different flow patterns. The input solar flux is introduced in the form of a step function and the resulting collector response is presented in each case. The numerical results of a selected example are plotted in Fig. 4 for comparison.
- 2 - Comparison of the exit temperature from the collector, Figure 4, indicates the distinct difference in responding to a sudden change of solar radiation. The outlet fluid temperature of flow pattern (1) responds by a much faster rate in the early stages since the fluid leaves the collector as soon as it absorbs the useful energy from the annulus area facing the sun. On the other hand, the fluid temperature of flow pattern (2) lags behind by the "residence" time. The latter is the time elapsed for an element of fluid to pass through the collector from the inlet section to the end section. The residence time θ_s is given by

$$\theta_s = \frac{L}{V}$$

and is equal to 8.46 minutes for this example. This means that approximately 8 minutes have to elapse to discharge the relatively colder fluid in the center tube before a significant temperature gain is observed for flow pattern (2).

- 3 - The steady state collector analysis, described in Ref. (1), leads to the conclusion that both flow patterns, though having different temperature distribution inside each tube, will eventually end up with the same steady state outlet fluid temperature. Since the temperature growth for

flow pattern (2) is lagging behind that of flow pattern (1) and catching up at some infinite time, the rate of temperature increase for flow pattern (2), at the end of the "residence" time has to be much faster than the early rate of response for flow pattern (1).

- 4 - The steady state time registered experimentally by the collector manufacturer and by the solar simulator team at NASA Lewis Research Center for this collector type, ranged from 30 to 60 minutes according to flow rates, ambient and solar flux conditions. This relatively long steady state time is due to the fact that 65% of the collector volume is filled with liquid fluid that hinders a fast response. The analytic results of the given example seem to agree with the above finding; the outlet fluid temperature reached 97% and 92.5% of its steady state value for flow patterns (1) and (2), respectively after 40 minutes of exposure to sudden solar radiation.
- 5 - The series solution presented in this work depends entirely on the parameters K_1 , C , L and V which in turn depends on the physical dimensions of the collector, the heat transfer coefficients and the fluid flow rate. With fixed collector dimensions, the higher the rate of fluid flowing in, the higher the conductance coefficients and the faster the response to solar flux changes will be, even though the useful temperature rise across the collector will decrease. On the other hand, with a fixed fluid flow rate, the smaller the area of the flow passage and the collector size, the higher the fluid velocity, the higher the conductance coefficients and the faster the rate of heating will be, since a smaller amount of liquid is residing inside the collector.

6 - The analytic solution can now be applied to different input conditions of flow rate, solar flux, ambient temperature or collector dimensions for optimizing the collector performance. Moreover, other step changes of the solar flux, such as sudden shading due to clouds passing by and their effects on the collector cooling rate, could be followed by the same expressions derived herein.

In conclusion, it should be pointed out that the analytic solutions obtained in this article could be handled with a digital computer to give adequate coverage for this type of solar collector.

Nomenclatures

A_{cs}	cross sectional area	m^2
C	specific heat of tube material	$Kwhr/Kg^{\circ}c$
C_f	specific heat of flowing fluid.	$Kwhr/Kg^{\circ}c$
D	Tube diameter	m
F	Augmented Radiation Factor	≥ 1
I	Direct incident solar radiation	Kw/m^2
j	$\sqrt{-1}$	
L	tube length	m
\dot{m}	fluid mass flow rate	Kg/hr
p	Laplacian frequency	
r	reflectivity	
\bar{T}	Transformed temperature on frequency domain	
T	Temperature	$^{\circ}K$
T_{sky}	Sky temperature	$^{\circ}K$
$T_{amb.}$	Ambient temperature	$^{\circ}K$
U_{ac}	Radiative heat transfer coefficient between the absorber and the cover tubes	$Kw/m^2^{\circ}c$
U_{ao}	Overall heat transfer coefficient between the absorber tube and the outer fluid in the annulus	$Kw/m^2^{\circ}c$
U_{cv}	convective heat transfer coefficient between the cover tube and the ambient air	$Kw/m^2^{\circ}c$
U_{oi}	overall heat transfer coefficient between the outer fluid and the inner fluid	$Kw/m^2^{\circ}c$
U_{rd}	Radiative heat transfer coefficient between the cover tube and sky.	$Kw/m^2^{\circ}c$
V	Fluid velocity.	m/hr
X	Distance along the collector tube	m

θ	Time
α	absorptivity
ϵ	emissivity
τ	transmissivity of cover tube
δ	tube thickness
σ	Stefan Boltzmann constant
ρ	density

Subscripts

a	absorber
c	cover tube
i	inner fluid, pass(1)
o	outer fluid, pass (2)

References

1. Lansing, F., "Heat Transfer Criteria of a Tubular Solar Collector - the Effect of Reversing the Flow Pattern on Collector Performance", Deep Space Network Progress Report 42-31, pp. 108-114, Jet Propulsion Laboratory, Pasadena, California, Feb. 15, 1976.
2. Rizika, J. W., "Thermal Lags in Flowing Incompressible Fluid Systems Containing Heat Capacitors", Trans. ASME, Vol, 78, 1956 pp. 1407-1413.
3. Cima, R. M. and London, A. L., "The Transient Response of a Two-fluid Counter Flow Heat Exchanger - The Gas Turbine Regenerator", Trans. ASME, Vol. 80, 1958, pp. 1169-1179.
4. London, A. L., Biancardi, F. R., and Mitchell, J. W., "The Transient Response of Gas-Turbine-Plant Heat Exchangers - Regenerators, Inter-coolers, Precoolers, and Ducting", Trans. ASME Series A, Journal of Engineering for Power, Vol. 81, 1959, pp. 433-448.
5. London, A. L., Sampsell, D. F., and McGowan, J. G., "The Transient Response of Gas Turbine Plant Heat Exchangers - Additional Solutions for Regenerators of the Periodic-Flow and Direct Transfer Types", Trans. ASME, Series A, Journal of Engineering for Power, Vol. 86, 1964, pp. 127-135.
6. Rohsenow, W. M., and Hartnett, J. P., "Handbook of Heat Transfer", McGraw Hill Book Co., N.Y., 1973, pp. 446-531.

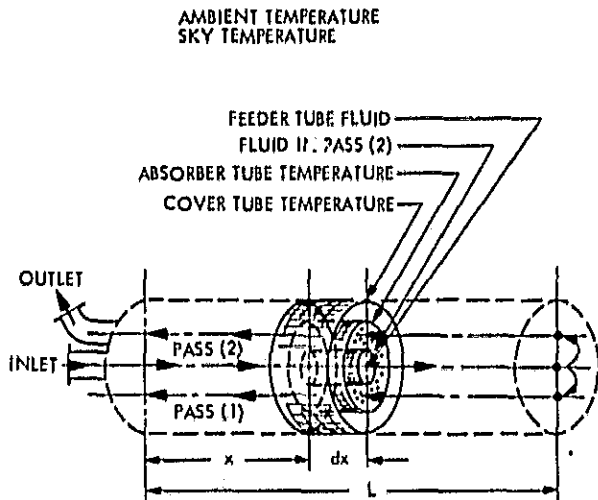


Fig. 1a. Collector configuration (flow pattern 1)

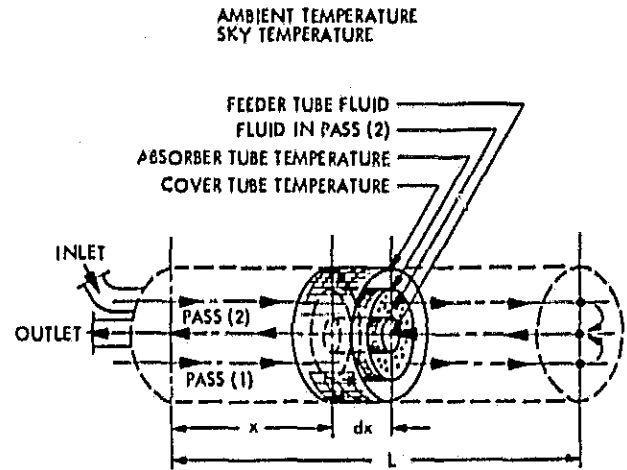


Fig. 2a. Collector configuration (flow pattern 2)

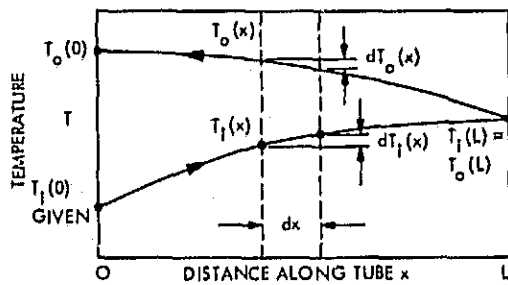


Fig. 1b. Temperature distribution along one collector (flow pattern 1) at time θ

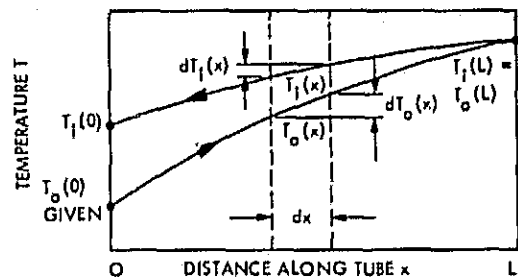


Fig. 2b. Temperature distribution along one collector (flow pattern 2) at time θ

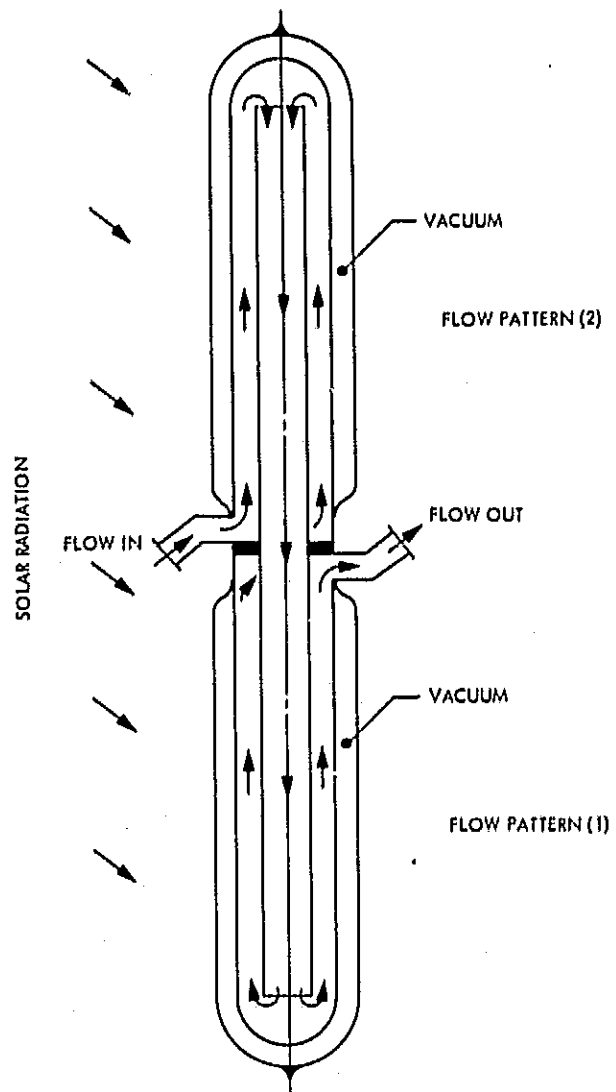


Fig. 3. Two collector tubes in series

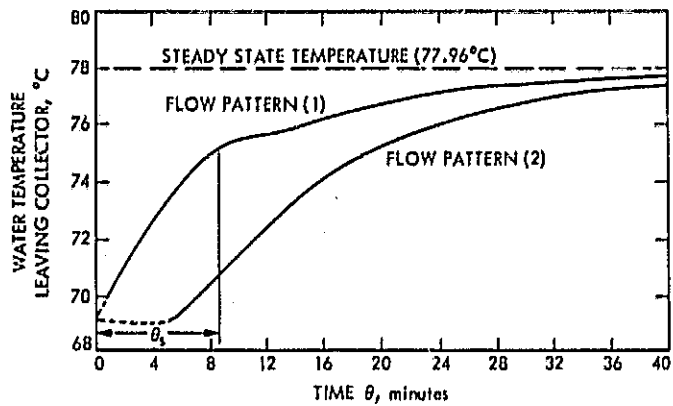


Fig. 4. Transient response of the outlet fluid temperature of the tubular solar collector as derived from the analysis

ORIGINAL PAGE IS
OF POOR QUALITY

Appendix A

Derivation of the system differential Equations for the Transient Solution

For a segment of the collector of length dx at the time interval from θ to $(\theta+d\theta)$, the rate of heat flux is divided, as shown in Figure A-1, whereby

dQ_1 = The total radiation on the cover tube from all sides including irradiancies from the back reflector and reflections from adjacent collectors;

$$dQ_1 = I \cdot F \cdot (D_c dx) \quad \dots (A-1)$$

dQ_2 = The total outward reflection loss from all sides of the cover tube,

dQ_3 = the energy absorbed by the cover tube including absorption from multiple reflections within the evacuated space

$$dQ_3 = \left(\alpha_c + \frac{\alpha_c r_a \tau_c}{1 - r_c r_a} \right) \cdot dQ_1 \quad \dots (A-2)$$

dQ_4 = the energy absorbed by the absorber tube including absorption from multiple reflections within the evacuated space,

$$dQ_4 = \left(\frac{\alpha_a \cdot \tau_c}{1 - r_c r_a} \right) \cdot dQ_1 \quad \dots (A-3)$$

dQ_5 = the long-wave radiation exchange between the cover and the absorber tubes. This is absorbed by the cover tube almost entirely.

$$dQ_5 = U_{ac} \cdot (\pi D_a dx) (T_a - T_c) \quad \dots (A-4)$$

where

$$\left. \begin{aligned} U_{ac} &= \sigma \cdot \epsilon_{ac} \cdot \frac{(T_a^4 - T_c^4)}{(T_a - T_c)} \\ \frac{1}{\epsilon_{ac}} &= \frac{1}{\epsilon_a} + \frac{D_a}{D_c} \left(\frac{1}{\epsilon_c} - 1 \right) \end{aligned} \right\} \quad \dots (A-5)$$

dQ_6 = the sensible heat gain by the absorber tube material

$$dQ_6 = \pi D_a \cdot \delta_a \cdot dx \cdot \rho_a \cdot c_a \left(\frac{\partial T_a}{\partial \theta} \right) \quad \dots (A-6)$$

dQ_7 = The heat transfer to the outer fluid in the annulus pass from the absorber tube surface

$$= U_{a0} \cdot (\pi D_a dx) \cdot (T_a - T_o) \quad \dots (A-7)$$

dQ_8 = The combined radiation and convection loss from the cover tube to the ambient air and sky.

$$dQ_8 = (\pi D_c dx) \cdot [U_{cv}(T_c - T_{amb}) + U_{rd}(T_c - T_{sky})] \quad \dots (A-8)$$

where

$$U_{rd} = \sigma \cdot \epsilon_c \cdot \left(\frac{T_c^4 - T_{sky}^4}{T_c - T_{sky}} \right) \quad \dots (A-9)$$

dQ_9 = The sensible heat gain by the cover tube material.

$$dQ_9 = \pi D_c \delta_c dx \cdot \rho_c \cdot C_c \left(\frac{\partial T_c}{\partial \theta} \right) \quad \dots (A-10)$$

dQ_{10} = The sensible heat gain by the outer fluid in the annulus pass. This is determined by the "Lagrangian" approach following the elementary fluid mass as it passes by the section bounded by X and $(X + dx)$ during the time interval from θ to $(\theta + d\theta)$

$$dQ_{10} = \left[A_{cs,2} \rho_f \cdot C_f \left(\frac{\partial T_o}{\partial \theta} \right) \mp \dot{m} C_f \left(\frac{\partial T_o}{\partial X} \right) \right] dx \quad \dots (A-11)$$

where the (-) sign is for flow pattern (1) and the (+) sign for flow pattern (2).

dQ_{11} = The heat transfer to the inner fluid,

$$dQ_{11} = U_{ci} (\pi D_i dx) \cdot (T_o - T_i) \quad \dots (A-12)$$

dQ_{12} = The sensible heat gain by the inner fluid, pass (1). This is determined, as in dQ_{10} , by following the elementary fluid mass as it passes by the section bounded by X and $(X + dx)$ during the time interval from θ to $(\theta + d\theta)$,

$$dQ_{12} = \left[A_{cs,1} \cdot \rho_f \cdot C_f \cdot \left(\frac{\partial T_i}{\partial \theta} \right) \pm \dot{m} C_f \left(\frac{\partial T_i}{\partial X} \right) \right] dx \quad \dots (A-13)$$

where the (+) sign is for flow pattern (1) and the (-) sign for flow pattern (2).

and

dQ_{13} = The sensible heat gain by the inner tube material.

Applying the first law of thermodynamics to the system componets will

yield:

$$dQ_3 + dQ_5 - dQ_8 - dQ_9 = 0 \quad \dots (A-14)$$

for the cover tube,

$$dQ_4 - dQ_5 - dQ_6 - dQ_7 = 0 \quad \dots (A-15)$$

for the absorber tube,

$$dQ_7 - dQ_{10} - dQ_{11} = 0 \quad \dots (A-16)$$

for the outer fluid, and

$$dQ_{11} - dQ_{12} - dQ_{13} = 0 \quad \dots (A-17)$$

for the inner fluid.

In this work, it has been assumed, without great loss of accuracy, that the heat capacitance of the three tubes of the collector are negligible relative to that of the liquid fluid. Accordingly, the number of differential equations decreases to two instead of four since

$$dQ_6 = dQ_9 = dQ_{13} = \text{zero} \quad \dots (A-18)$$

and equations A-14 and A-15 are reduced to:

$$\begin{aligned} & \left[\left(\alpha_c + \frac{\alpha_c r_a \tau_c}{1 - r_a r_c} \right) \cdot \text{I.F.} (D_c dx) \right] + \left[(\pi D_a dx) \cdot U_{ac} \cdot (T_a - T_c) \right] \\ & - \pi D_c dx \left[U_{cv} (T_c - T_{amb}) + U_{rd} (T_c - T_{sky}) \right] = 0 \\ & \left[\left(\frac{\alpha_a \tau_c}{1 - r_a r_c} \right) \cdot \text{I.F.} (D_c dx) \right] - \left[(\pi D_a dx) \cdot U_{ac} (T_a - T_c) \right] - \\ & - \left[(\pi D_a dx) \cdot U_{ao} \cdot (T_a - T_o) \right] = 0 \end{aligned}$$

These can be written as:

$$\left. \begin{aligned} T_c &= a + b T_a \\ T_c &= f T_a - (f-1) T_o - g \end{aligned} \right\} \dots (A-19)$$

where a , b , f & g are characteristic constants given by:

$$\left. \begin{aligned} a &= \frac{\left[\left(\alpha_c + \frac{\alpha_a r_a \tau_c}{1-r_a r_c} \right) \frac{F \cdot I}{\pi} + (U_{cv} \cdot T_{amb} + U_{rd} T_{sky}) \right]}{\left[U_{cv} + U_{rd} + \left(\frac{D_a}{D_c} \cdot U_{ac} \right) \right]} \\ b &= \frac{\left(\frac{D_a}{D_c} \cdot U_{ac} \right)}{\left(U_{cv} + U_{rd} + \frac{D_a}{D_c} \cdot U_{ac} \right)} \end{aligned} \right\} \dots (A-20)$$

$$f = \left(1 + \frac{U_{ao}}{U_{ac}} \right), \quad g = \frac{F \cdot I}{\pi \left(U_{ac} \cdot \frac{D_a}{D_c} \right)} \left(\frac{\alpha_a \tau_c}{1-r_a r_c} \right)$$

On the other hand, Equations A-16 and A-17 will become the two governing differential equations written as

$$\begin{aligned} & [U_{ao} \cdot (\pi D_a dx) \cdot (T_a - T_o)] - [U_{oi} (\pi D_i dx) (T_o - T_i)] - \\ & - \left[A_{cs2} \rho_f C_f \frac{\partial T_o}{\partial \theta} \mp \dot{m} C_f \frac{\partial T_o}{\partial x} \right] dx = 0 \end{aligned}$$

where the (-) sign is for flow pattern (1) and the (+) sign for flow pattern (2),

$$[U_{oi} (\pi D_i dx) (T_o - T_i)] - \left[A_{cs1} \rho_f C_f \left(\frac{\partial T_i}{\partial \theta} \right) \pm \dot{m} C_f \left(\frac{\partial T_i}{\partial x} \right) \right] dx = 0$$

where the (-) sign is for flow pattern (1) and the (+) sign for flow pattern (2).

The continuity (mass conservation) equation is expressed as:

$$\dot{m} = \rho_f A_{cs1} \cdot V_i = \rho_f A_{cs2} \cdot V_o \dots (A-21)$$

And together with Equations A-19 and A-20, the simultaneous partial differential equations governing the thermal behavior of the tubular solar collector are expressed as:

$$\left. \begin{aligned} \pm \frac{\partial T_i}{\partial X} + \frac{1}{V_i} \frac{\partial T_i}{\partial \theta} + K_1 T_i - K_1 T_o &= 0 \\ \pm \frac{\partial T_o}{\partial X} - \frac{1}{V_o} \frac{\partial T_o}{\partial \theta} + K_1 T_i - K_3 T_o + K_4 &= 0 \end{aligned} \right\} \dots (A-22)$$

where

$$\left. \begin{aligned} K_1 &= \frac{\pi D_i U_{oi}}{m C_f} , & K_2 &= \frac{\pi D_a U_{ao}}{m C_f} \\ K_3 &= K_1 + K_2 \left(\frac{1-b}{f-b} \right) \\ K_4 &= K_2 \left(\frac{a+g}{f-b} \right) \end{aligned} \right\} \dots (A-23)$$

the (+) sign is for flow pattern (1) and the (-) sign is for flow pattern (2).

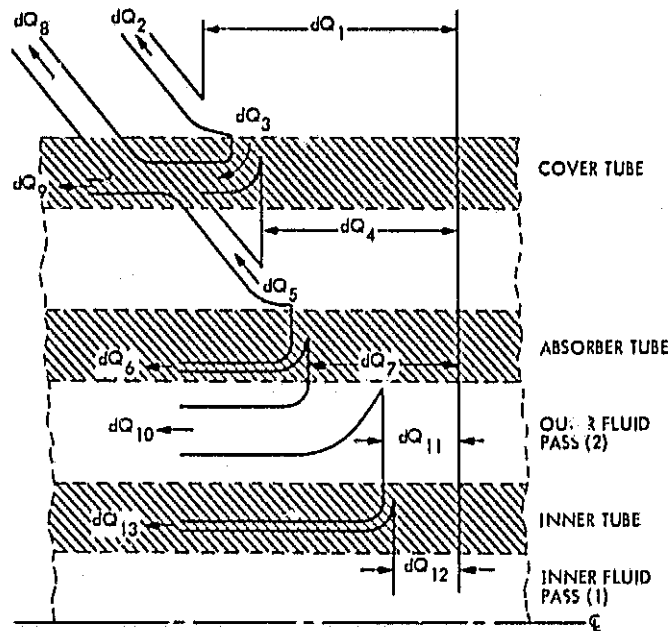


Fig. A-1. Sankey Diagram for the Tubular Solar Collector

ORIGINAL PAGE IS
OF POOR QUALITY

Appendix B

Transformation of the differential equations from the time domain to the frequency domain.

The partial differential equations that govern the collector inner and outer fluid temperatures $T_i(X, \theta)$ and $T_o(X, \theta)$, respectively, are expressed as

$$\left. \begin{aligned} \pm \frac{\partial T_i}{\partial X} + \frac{1}{V} \frac{\partial T_i}{\partial \theta} + K_1 T_i - K_1 T_o &= 0 \\ \pm \frac{\partial T_o}{\partial X} - \frac{1}{V} \frac{\partial T_o}{\partial \theta} + K_1 T_i - K_3 T_o + K_4 &= 0 \end{aligned} \right\} \dots (B-1)$$

where K_1 , K_3 , & K_4 are characteristic parameters, and

$$V_i = V_o = V \dots (B-2)$$

according to the ninth assumption in the main text. The (+) sign is for flow pattern (1) and the (-) sign for flow pattern (2). At steady state conditions, the above set of equations are reduced to the same set derived in Ref. (1), namely

$$\left. \begin{aligned} \pm \frac{d^2 T_i}{dx^2} + K_1 T_i - K_1 T_o &= 0 \\ \pm \frac{d^2 T_o}{dx^2} + K_1 T_i - K_3 T_o + K_4 &= 0 \end{aligned} \right\} \dots (B-3)$$

where the (+) sign is for flow pattern (1) and the (-) sign for flow pattern (2).

The following Laplace transforms will convert the set of equations in (B-1) from the time θ domain to the frequency p domain to ease their algebraic manipulation. These are

$$\left. \begin{aligned} \bar{T}_i(X, P) &= \int_0^{\infty} e^{-p\theta} T_i(X, \theta) d\theta \\ \bar{T}_o(X, P) &= \int_0^{\infty} e^{-p\theta} T_o(X, \theta) d\theta \end{aligned} \right\} \dots (B-4)$$

Multiplying equation (B-1) by $e^{-p\theta}$ and integrating from $(\theta=0)$ to $(\theta=\infty)$ gives:

$$\left. \begin{aligned} \pm \frac{\partial \bar{T}_i}{\partial X} + (K_1 + \frac{P}{V}) \bar{T}_i - K_1 \bar{T}_0 - \frac{T_i(X,0)}{V} &= 0 \\ \pm \frac{\partial \bar{T}_0}{\partial X} - (K_3 + \frac{P}{V}) \bar{T}_0 + K_1 \bar{T}_i + \frac{K_4}{P} + \frac{T_0(X,0)}{V} &= 0 \end{aligned} \right\} \dots (B-5)$$

where the (+) sign is for flow pattern (1) and the (-) sign for flow pattern (2). The two simultaneous partial differential equations could be separated for either variable by using Cramer's rule. These are expressed as

$$\begin{aligned} \frac{\partial^2 \bar{T}_i}{\partial X^2} \mp (K_3 - K_1) \frac{\partial \bar{T}_i}{\partial X} - [(K_1 + \frac{P}{V})(K_3 + \frac{P}{V}) - K_1^2] \bar{T}_i + K_1 (\frac{K_4}{P} + \frac{T_0(X,0)}{V}) \\ + [\frac{T_i(X,0)}{V} \cdot (K_3 + \frac{P}{V})] \mp \frac{1}{V} \frac{\partial T_i}{\partial X}(X,0) = 0 \end{aligned} \dots (B-6)$$

and

$$\begin{aligned} \frac{\partial^2 \bar{T}_0}{\partial X^2} \mp (K_3 - K_1) \frac{\partial \bar{T}_0}{\partial X} - [(K_1 + \frac{P}{V})(K_3 + \frac{P}{V}) - K_1^2] \bar{T}_0 \\ = -K_1 \cdot \frac{T_i(X,0)}{V} - [(K_1 + \frac{P}{V})(\frac{K_4}{P} + \frac{T_0(X,0)}{V})] \mp \frac{1}{V} \cdot \frac{\partial T_0(X,0)}{\partial X} \end{aligned} \dots (B-7)$$

where the (-) sign is for flow pattern (1) and the (+) sign for flow pattern (2).

i - Initial Temperature Distribution Along the Tube at $\theta = 0$

This step has to be determined first before a general solution can be made. Generally speaking, the initial conditions are arbitrarily preassigned based on past experience. However, in this work there is no need for any initial estimates or guesses since we have already stated in the seventh assumption in the main text that initial conditions are at steady state. Accordingly, using equation (B-3), the initial temperatures $T_i(X,0)$ and $T_o(X,0)$ are related by:

$$\left. \begin{aligned} \pm \frac{\partial T_i(X,0)}{\partial X} + K_1 T_i(X,0) - K_1 T_o(X,0) &= 0 \\ \pm \frac{\partial T_o(X,0)}{\partial X} + K_1 T_i(X,0) - K_3 T_o(X,0) + K_4(0) &= 0 \end{aligned} \right\} \dots (B-8)$$

where the (+) sign is for flow pattern (1) and the (-) sign for flow patterns (2). Equation B-8 can be further separated for one of the temperatures $T_i(X,0)$ or $T_o(X,0)$ as:

$$\frac{d^2 T_i \text{ (or } T_o)}{dx^2} \mp (K_3 - K_1) \frac{dT_i \text{ (or } T_o)}{dx} - K_1 (K_3 - K_1) = -K_1 K_4(0) \dots (B-9)$$

where the (-) sign is for flow pattern (1) and the (+) sign for flow pattern (2). For each flow pattern, equation B-9 is solved subject to the boundary conditions at the end ($X=L$) as reported in Ref. (1). The result is an explicit relationship for the quantities $T_i(X,0)$, $T_o(X,0)$, $\frac{dT_i(X,0)}{dx}$ and $\frac{dT_o(X,0)}{dx}$ with the distance X along the tube.

ii - General Solution in the p-plane:

Our interest in this work is to study the thermal response when a sudden step change in the insolation "I" is imposed. Figures B-1 and B-2 illustrate the resulting change in the parameter $K_4(0)$. The latter can be written as

$$K_4(\theta) = K_4(0) + \Delta K_4 \cdot v(0) \quad \dots (B-10)$$

where $v(0)$ is the unit step function at $\theta = 0$.

Substituting the initial conditions given by equation (B-8) in equations (B-6) and (B-7), will give

$$\begin{aligned} \frac{\partial^2 \bar{T}_i}{\partial X^2} \mp (K_3 - K_1) \frac{\partial \bar{T}_i}{\partial X} - \left[(K_1 + \frac{P}{V})(K_3 + \frac{P}{V}) - K_1^2 \right] \bar{T}_i \\ = - \frac{K_1 K_4}{p} - \frac{T_i(X,0)}{V} (K_1 + K_3 + \frac{P}{V}) \quad \dots (B-11) \end{aligned}$$

and

$$\begin{aligned} \frac{\partial^2 \bar{T}_o}{\partial X^2} \mp (K_3 - K_1) \frac{\partial \bar{T}_o}{\partial X} - \left[(K_1 + \frac{P}{V})(K_3 + \frac{P}{V}) - K_1^2 \right] \bar{T}_o \\ = - \frac{K_1 K_4}{p} - \frac{T_o(X,0)}{V} (K_1 + K_3 + \frac{P}{V}) - \frac{\Delta K_4}{V} \quad \dots (B-12) \end{aligned}$$

where the (-) sign is for flow pattern (1) and the (+) sign for flow pattern (2).

The particular "integral" or solution can thus be determined from equations (B-11) and (B-12) as

$$\left\{ \frac{T_i(X,0)}{p} + \frac{K_1 \Delta K_4 V^2}{p(p+r_1)(p+r_2)} \right\}$$

for $\bar{T}_i(X,p)$ and both flow patterns,

and for $\bar{T}_o(X,p)$ the particular "integral" is given by

$$\left\{ \frac{T_o(X,0)}{p} + \frac{K_1 \Delta K_4 V^2}{p(p+r_1)(p+r_2)} + \frac{\Delta K_4 V}{(p+r_1)(p+r_2)} \right\}$$

for both flow patterns where

$$\left[\left(K_1 + \frac{P}{V} \right) \left(K_3 + \frac{P}{V} \right) - K_1^2 \right] = \frac{1}{V^2} (p+r_1)(p+r_2) \quad \dots (B-13)$$

is written for simplifying the inverse transformation

and

$$\left. \begin{aligned} r_1 r_2 &= 2CV^2 K_1, & (r_1+r_2) &= 2(C+K_1)V, & C &= \frac{(K_3-K_1)}{2} \\ r_1 &= CV + K_1V + V\sqrt{C^2 + K_1^2} \\ r_2 &= CV + K_1V - V\sqrt{C^2 + K_1^2} \end{aligned} \right\} \dots (B-14)$$

On the other hand, the roots of the "characteristic" equation of the image differential equations (B-11) and (B-12) are such that

$$\bar{S}_{1,2}^2 \mp \bar{S}_{1,2} (K_3-K_1) - \left[\left(K_1 + \frac{P}{V} \right) \left(K_3 + \frac{P}{V} \right) - K_1^2 \right] = 0 \quad \dots (B-15)$$

where the (-) sign is for flow pattern (1) and the (+) sign for flow pattern (2).

The roots $\bar{S}_1(p)$ and $\bar{S}_2(p)$ are further written in the form:

$$\left. \begin{aligned} \bar{S}_1(p) &= \pm (C + R) \\ \bar{S}_2(p) &= \pm (C - R) \\ R &= \sqrt{\left(\frac{P}{V} + C \right) \left(\frac{P}{V} + C + 2K_1 \right)} \end{aligned} \right\} \dots (B-16)$$

where the (+) sign is for flow pattern (1) and the (-) sign for flow pattern (2).

The general solution for $\bar{T}_i(X,p)$ and $\bar{T}_0(X,p)$ is given by:

$$\bar{T}_i(X,p) = A_1(p) \bar{S}_1 X + A_2(p) \frac{\bar{S}_2 X}{e^{\bar{S}_2 X}} + \frac{T_i(X,0)}{p} + \frac{K_1 V^2 \Delta K_4}{p(p+r_1)(p+r_2)} \quad \dots (B-17)$$

$$\bar{T}_0(X,p) = A_3(p) \bar{S}_1^X + A_4(p) \bar{S}_2^X + \frac{T_0(X,0)}{p} + \frac{K_1 v^2 \Delta K_4}{p(p+r_1)(p+r_2)} + \frac{\Delta K_4 v}{(p+r_1)(p+r_2)} \dots (B-18)$$

where $A_1(p)$, $A_2(p)$, $A_3(p)$ and $A_4(p)$ are arbitrary functions of the frequency p . Substituting in any one of the image differential equations such as equation B-5, and comparing the coefficients of exponential and absolute terms:

$$\left. \begin{aligned} A_3(p) &= \frac{A_1(p)}{K_1} (K_1 + C + \frac{p}{V} + R) \\ A_4(p) &= \frac{A_2(p)}{K_1} (K_1 + C + \frac{p}{V} - R) \end{aligned} \right\} \dots (B-19)$$

for both flow patterns.

Combining equations B-16, B-17, B-18 and B-19 gives

$$\bar{T}_i(X,p) = A_1(p) \bar{S}_1^X + A_2(p) \bar{S}_2^X + \frac{T_i(X,0)}{p} + \frac{K_1 \Delta K_4 v^2}{p(p+r_1)(p+r_2)} \dots (B-20)$$

$$\begin{aligned} \bar{T}_0(X,p) &= \frac{A_1(p)}{K_1} (K_1 + C + \frac{p}{V} + R) e^{\bar{S}_1 X} + \frac{A_2(p)}{K_1} (K_1 + C + \frac{p}{V} - R) e^{\bar{S}_2 X} \\ &+ \frac{T_0(X,0)}{p} + \frac{K_1 \Delta K_4 v^2}{p(p+r_1)(p+r_2)} + \frac{\Delta K_4 v}{(p+r_1)(p+r_2)} \dots (B-21) \end{aligned}$$

for both flow patterns except for the signs of \bar{S}_1 and \bar{S}_2 .

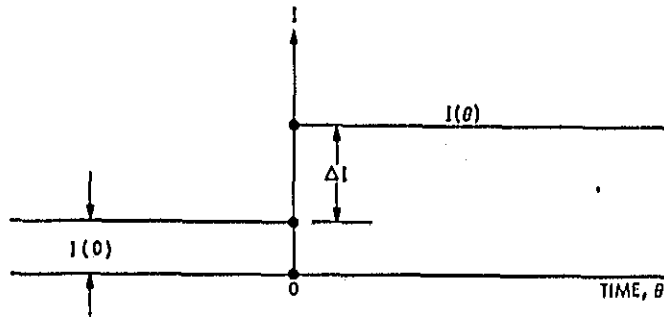


Fig. B-1. Step change in the solar radiation at $\theta = 0$.

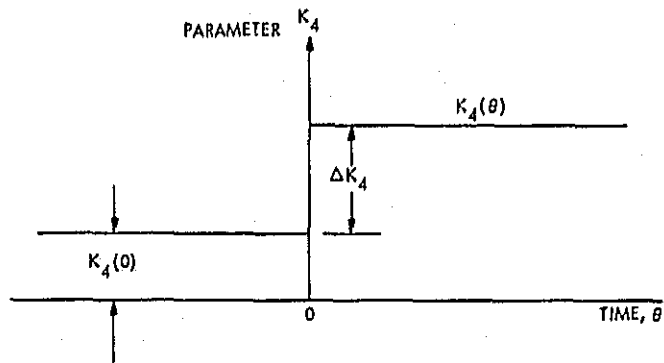


Fig. B-2. Step change in the parameter K_4

Appendix C

Inverse Transformation from the Frequency Domain to the Time Domain for Flow Pattern (1).

1 - Boundary and Initial Conditions:

With the image temperatures $\bar{T}_i(X,p)$ and $\bar{T}_o(X,p)$ as determined from Appendix B, equations B-20 and B-21 are subject to the following two conditions:

1. A boundary condition:

At $X = L$ and at all times:

$$T_i(L,\theta) = T_o(L,\theta)$$

or

$$\bar{T}_i(L,p) = \bar{T}_o(L,p) \quad \dots(C-1)$$

2. An initial condition:

At the inlet section ($X=0$) and at all times, the temperature $T_i(0,\theta)$ is kept fixed, i.e.,

$$T_i(0,\theta) = T_i(0,0) = \text{constant}$$

or

$$\bar{T}_i(0,p) = \frac{T_i(0,0)}{p} \quad \dots(C-2)$$

The arbitrary constants $A_1(p)$ and $A_2(p)$ for flow pattern (1) are then given by:

$$A_1(p) = \frac{K_1 \Delta K_4 \cdot V^2}{p(p+r_1)(p+r_2)} \frac{\left[(\bar{S}_2 + \frac{p}{V}) \bar{S}_2^L - \frac{p}{V} \right]}{\left[(\bar{S}_1 + \frac{p}{V}) \bar{S}_1^L - (\bar{S}_2 + \frac{p}{V}) \bar{S}_2^L \right]}$$

$$A_2(p) = \frac{-K_1 \Delta K_4 \cdot V^2}{p(p+r_1)(p+r_2)} \frac{\left[(\bar{S}_1 + \frac{p}{V}) \bar{S}_1^L - \frac{p}{V} \right]}{\left[(\bar{S}_1 + \frac{p}{V}) \bar{S}_1^L - (\bar{S}_2 + \frac{p}{V}) \bar{S}_2^L \right]} \quad \dots(C-3)$$

where

$$\left. \begin{aligned} \bar{S}_1(p) &= (C + R) \quad , \\ \bar{S}_2(p) &= (C - R) \quad , \\ R &= \sqrt{\left(\frac{P}{V} + C\right)\left(\frac{P}{V} + C + 2K_1\right)} \end{aligned} \right\} \dots (C-4)$$

and r_1, r_2 are given by Equation B-14.

ii - Poles on the Complex Plane

The straightforward process of finding the poles or "singular points" of the transformed temperatures $\bar{T}_i(X,p)$ and $\bar{T}_o(X,p)$ and following it by application of the "residues" theorem, is the fastest procedure to solve for the inverse Laplace transformation.

The values of p which result in an infinite value for $\bar{T}_i(X,p)$ or $\bar{T}_o(X,p)$ are herein called the poles and given by

$$(1) \ p_1=0, \quad (2) \ p_2=-r_1, \quad (3) \ p_3=-r_2, \quad \text{and} \quad (4) \ p_4= p_m$$

where p_m is an infinite set of complex poles that satisfy the equation

$$\left. \begin{aligned} \left(C + \frac{p_m}{V} + R_m\right) e^{R_m L} &= \left(C + \frac{p_m}{V} - R_m\right) e^{-R_m L} \\ R_m &= \sqrt{\left(\frac{p_m}{V} + C\right)\left(\frac{p_m}{V} + C + 2K_1\right)} \end{aligned} \right\} \dots (C-5)$$

Since $\bar{T}_i(X,p)$ and $\bar{T}_o(X,p)$ are analytic everywhere in the region including the simple poles listed above, then the inverse transformation $T(X,\theta)$ is given by the sum of residues of $\left[e^{p\theta} \bar{T}(X,p) \right]$ at the poles of $\bar{T}(X,p)$.

iii - Residues of the term $\left[A_1(p) \bar{S}_1^X + A_2(p) \bar{S}_2^X \right]$:

This term appears in Equations B-20 and B-21 for the image temperatures \bar{T}_1 and \bar{T}_0 , respectively. It can be written as:

$$\left[A_1(p) \bar{S}_1^X + A_2(p) \bar{S}_2^X \right] = \frac{K_1 \Delta K_4 V^2 \left\{ e^{(C+R)X} \left[(C+\frac{p}{V} - R) e^{-\frac{(C-R)L}{V}} - \frac{p}{V} \right] - e^{(C-R)X} \left[(C+\frac{p}{V}+R) e^{-\frac{(C+R)L}{V}} - \frac{p}{V} \right] \right\}}{p(p+r_1)(p+r_2) \left\{ (C+\frac{p}{V}+R) e^{(C+R)L} - (C+\frac{p}{V} - R) e^{(C-R)L} \right\}} \dots (C-6)$$

The corresponding residue to each pole is listed as follows:

(1) Residue at the Pole: $p = 0$

This represents the steady state value of this term and is given by

$$\text{residue}_{(p=0)} = \frac{-\Delta K_4}{2C} \frac{CX}{e} \frac{\left\{ C \sinh R_1(L-X) + R_1 \cosh R_1(L-X) \right\}}{(C \sinh R_1 L + R_1 \cosh R_1 L)} \dots (C-7)$$

$$\text{where } R_1 = \sqrt{C(C+2K_1)}$$

(2) Residue at the pole: $p = -r_1$

This is given by

$$\text{residue}_{(p=-r_1)} = \frac{K_1 \Delta K_4 V^2}{r_1(r_2-r_1)} \cdot e^{-r_1 X} \dots (C-8)$$

independent of the distance X .

(3) Residue at the pole: $p = -r_2$

This is given by

$$\text{residue}_{(p=-r_2)} = \frac{-K_1 \Delta K_4 V^2}{r_2(r_2-r_1)} \cdot e^{-r_2 X} \dots (C-9)$$

independent of the distance X .

(4) Residues at the set of complex poles p_m :

This is given by

$$\sum_m \frac{K_1 \Delta K_4 \cdot e^{p_m \theta} \cdot R_m \left[\frac{V}{p_m} - \frac{1}{(C + \frac{p_m}{V} + R_m)} \frac{(C+R_m)L}{e^{(C+R_m)L}} \right] \left[\frac{(C+R_m)^X}{e^{(C+R_m)^X}} - \frac{(C-R_m)^X}{e^{(C-R_m)^X}} \right]}{\left\{ 1 + 2L \left(\frac{p_m}{V} + C + K_1 \right) \right\} (R_m^2 - C^2)} \dots (C-10)$$

which is reduced to zero at the section $X=0$.

iv - Residues of the term $\left[\frac{A_1(p)}{K_1} (C + \frac{p}{V} + R) e^{\bar{S}_1 X} + \frac{A_2(p)}{K_1} (C + \frac{p}{V} - R) e^{\bar{S}_2 X} \right]$

This term appears in Equation B-21 for the image temperature \bar{T}_0 and is written as:

$$= \frac{\Delta K_4 V^2 \left\{ e^{(C-R)X} \left[2K_1 (C + \frac{p}{V}) e^{(C+R)L} + \frac{p}{V} (C + \frac{p}{V} - R) \right] - e^{(C+R)X} \left[2K_1 (C + \frac{p}{V}) e^{(C-R)L} + \frac{p}{V} (C + \frac{p}{V} + R) \right] \right\}}{p(p+r_1)(p+r_2) \cdot \left[(C + \frac{p}{V} + R) e^{(C+R)L} - (C + \frac{p}{V} - R) e^{(C-R)L} \right]} \dots (C-11)$$

The corresponding residue to each pole is listed as follows:

(1) Residue at the pole $p = 0$:

This represents the steady state value of this term and is given by:

$$\text{residue} = \frac{\Delta K_4 \cdot e^{CX} \cdot \sinh(L-X) R_1}{(C \sinh R_1 L + R_1 \cosh R_1 L)} \dots (C-12)$$

where

$$R_1 = \sqrt{C(C+2K_1)}$$

(2) Residue at the pole $p = -r_1$

This is given by

$$\text{residue} = \frac{-\Delta K_4 V e^{-r_1 \theta}}{(r_2 - r_1)} \dots (C-13)$$

independent of the distance X .

(3) Residue at the pole $p = -r_2$:

This is given by

$$\text{residue} = \frac{\Delta K_4 V e^{-r_2 \theta}}{(p = -r_2) (r_2 - r_1)} \dots (C-14)$$

independent of the distance X .

(4) Residue at the set of complex poles p_m :

This is given by

$$\sum_m \frac{\Delta K_4 \cdot R_m e^{p_m \theta} \left\{ \frac{V}{p_m} - \frac{1}{(C + \frac{p_m}{V} + R_m) e^{(C+R_m)L}} \right\} \left\{ e^{(C+R_m)X} \cdot (C + \frac{p_m}{V} + R_m) - e^{(C-R_m)X} (C + \frac{p_m}{V} - R_m) \right\}}{(R_m^2 - C^2) \left\{ 1 + 2L \left(\frac{p_m}{V} + C + K_1 \right) \right\}} \dots (C-15)$$

v - Special Solution at Section $X=0$

Combining Equations C-7, 8, 9, 10, 12, 13, 14 and 15 and substituting $X=0$

then

$$T_1(0, \theta) = T_i(0, 0) = \text{constant}$$

$$T_0(0, \theta) = T_0(0, 0) + \frac{\Delta K_4 \tanh R_1 L}{(C \tanh R_1 L + R_1)} + \sum_m \frac{2 \Delta K_4 e^{p_m \theta} R_m^2 \left\{ \frac{V}{p_m} - \frac{1}{(C + \frac{p_m}{V} + R_m) e^{(C+R_m)L}} \right\}}{(R_m^2 - C^2) \left\{ 1 + 2L \left(\frac{p_m}{V} + C + K_1 \right) \right\}} \dots (C-16)$$

*Inverse Laplace transform of $\frac{\Delta K_4 V}{(p+r_1)(p+r_2)} = \frac{\Delta K_4 V}{(r_2-r_1)} (e^{-r_1 \theta} - e^{-r_2 \theta})$

and

Inverse Laplace transform of $\frac{\Delta K_4}{p(p+r_1)(p+r_2)} = \frac{\Delta K_4}{2C} - \frac{\Delta K_4 K_1 V^2}{r_1(r_2-r_1)} e^{-r_1 \theta} + \frac{\Delta K_4 K_1 V^2}{r_2(r_2-r_1)} e^{-r_2 \theta}$

vi - Determination of the set of complex poles p_m

The infinite set of poles p_m that satisfy equation C-5 can be found numerically by solving for the complex number Z such that

$$\sinh^2 Z = \frac{Z^2}{4L^2 K_1^2} \quad ; \quad Z = 2LR_m \quad \dots (C-17)$$

where $Z = Z_x + jZ_y$ is a complex number. The components Z_x and Z_y are determined by solving numerically the following simultaneous equations:

$$\left. \begin{aligned} 2LK_1 \sinh Z_x \cos Z_y - Z_x &= 0 \\ 2LK_1 \cosh Z_x \sin Z_y - Z_y &= 0 \end{aligned} \right\} \quad \dots (C-18)$$

The roots of Equation C-18 are only functions of the constants L and K_1 ; and independent of the distance X. The sets p_m and R_m can thus be followed from Equations (C-5) and (C-17).

Appendix D

Inverse transformation from the frequency domain to the time domain for flow pattern (2).

i - Boundary and Initial Conditions

With the image temperatures $\bar{T}_i(X,p)$ and $\bar{T}_o(X,p)$ as determined from Appendix B, Equations B-19 and B-20 are subject to the following two conditions:

(1) A boundary condition:

At $(X = L)$ and at all times

$$T_i(L,\theta) = T_o(L,\theta)$$

or

$$\bar{T}_i(L,p) = \bar{T}_o(L,p) \quad \dots(D-1)$$

(2) An initial condition:

At the inlet section $(X=0)$ and at all times, the temperature $T_o(0,\theta)$ is kept fixed, i.e.,

$$T_o(0,\theta) = T_o(0,0) = \text{constant}$$

or

$$\bar{T}_o(0,p) = \frac{T_o(0,0)}{p} \quad \dots(D-2)$$

The arbitrary constants $A_1(p)$ and $A_2(p)$ for flow pattern: (2) are then given by:

$$A_1(p) = \frac{\Delta K_4 V^2}{p(p+r_1)(p+r_2)} \left\{ \frac{(C+\frac{P}{V}-R)(\frac{P}{V}+K_1) e^{(R-C)L} - \frac{P}{V}(K_1+C+\frac{P}{V}-R)}{e^{-CL} \left[(C+\frac{P}{V}+R) e^{RL} - (C+\frac{P}{V}-R) e^{-RL} \right]} \right\} \quad \dots(D-3)$$

$$A_2(p) = \frac{-\Delta K_4 V^2}{p(p+r_1)(p+r_2)} \left\{ \frac{(C+\frac{P}{V}+R)(\frac{P}{V}+K_1) e^{-(C+R)L} - \frac{P}{V}(K_1+C+\frac{P}{V}+R)}{e^{-CL} \left[(C+\frac{P}{V}+R) e^{RL} - (C+\frac{P}{V}-R) e^{-RL} \right]} \right\}$$

where $R = \sqrt{\left(\frac{P}{V}+C\right)\left(\frac{P}{V}+C+2K_{11}\right)}$

ii - Poles on the complex plane:

The values of p that lead to infinite values for \bar{T}_i or \bar{T}_o are identical to those found in Appendix C for flow pattern (1).

iii - Residues of the term $\left(A_1(p) e^{-(C+R)X} + A_2(p) e^{-(C-R)X} \right)$:

This can be written as:

$$\frac{\Delta K_4 V^2 \cdot e^{-X(C+R)} \left[\left(C + \frac{P}{V} - R \right) \left(\frac{P}{V} + K_1 \right) e^{(R-C)L} - \frac{P}{V} \left(K_1 + C + \frac{P}{V} - R \right) \right]}{p(p+r_1)(p+r_2) \left[\left(C + \frac{P}{V} + R \right) e^{RL} - \left(C + \frac{P}{V} - R \right) e^{-RL} \right]} e^{-CL}$$

$$\frac{\Delta K_4 V^2 \cdot e^{(R-C)X} \left[\left(C + \frac{P}{V} + R \right) \left(\frac{P}{V} + K_1 \right) e^{-(C+R)L} - \frac{P}{V} \left(K_1 + C + \frac{P}{V} + R \right) \right]}{p(p+r_1)(p+r_2) \left[\left(C + \frac{P}{V} + R \right) e^{RL} - \left(C + \frac{P}{V} - R \right) e^{-RL} \right]} e^{-CL} \quad \dots (D-4)$$

(1) Residue at the pole $p = 0$:

This represents the steady state value of this term and is given by

$$= \frac{\Delta K_4}{2C} e^{-CX} \frac{\left\{ C \sinh R_1(L-X) - R_1 \cosh R_1(L-X) \right\}}{\left(C \sinh R_1 L + R_1 \cosh R_1 L \right)}$$

at $X = 0$ this is reduced to

$$\text{residue} = \frac{\Delta K_4 \tanh R_1 L}{\left(C \tanh R_1 L + R_1 \right)} - \frac{\Delta K_4}{2C} \quad \dots (D-5)$$

(2) Residue at the pole $p = -r_1$

This is given by:

$$\text{residue} = \frac{\Delta K_4 \cdot K_1 V^2}{r_1(r_2 - r_1)} e^{-r_1 \theta} \quad \dots (D-6)$$

independent of the distance X .

(3) Residue at the pole $p = -r_2$:

This is given by:

$$\text{residue}_{(p=-r_2)} = \frac{-\Delta K_4 K_1 V^2}{r_2(r_2-r_1)} e^{-r_2 \theta} \quad \dots (D-7)$$

independent of the distance X .

(4) Residue at the set of complex poles p_m :

This is given by:

$$\sum_m \frac{\Delta K_4 R_m e^{p_m \theta}}{(R_m^2 - C^2) \left(1 + 2L \left(\frac{p_m}{V} + C + K_1\right)\right)} \cdot e^{-(C+R_m)X} \left\{ \left(1 + \frac{K_1 V}{p_m}\right) e^{2R_m L} - \frac{\left(K_1 + \frac{p_m}{V} + C - R_m\right)}{e^{(R_m-C)L} \left(C + \frac{p_m}{V} + R_m\right)} \right\}$$

$$- \sum_m \frac{\Delta K_4 R_m e^{p_m \theta}}{(R_m^2 - C^2) \left(1 + 2L \left(\frac{p_m}{V} + C + K_1\right)\right)} \cdot e^{(R_m-C)X} \left\{ \left(1 + \frac{K_1 V}{p_m}\right) e^{-2R_m L} - \frac{\left(K_1 + \frac{p_m}{V} + C + R_m\right)}{e^{(R_m-C)L} \left(C + \frac{p_m}{V} + R_m\right)} \right\}$$

... (D-8)

iv - Special solution at $X = 0$.

$$T_i(0, \theta) = T_i(0, 0) + \left(\frac{\Delta K_4 \tanh R_1 L}{C \tanh R_1 L + R_1} \right)$$

$$+ \sum_m \frac{2 \Delta K_4 \cdot e^{p_m \theta} R_m^2}{(R_m^2 - C^2) \left\{ 1 + 2L \left(\frac{p_m}{V} + C + K_1\right) \right\}} \cdot \left\{ \frac{1}{e^{(R_m-C)L} \cdot \left(C + \frac{p_m}{V} + R_m\right)} + \left(\frac{V}{p_m} + \frac{1}{K_1}\right) \right\}$$

... (D-9)